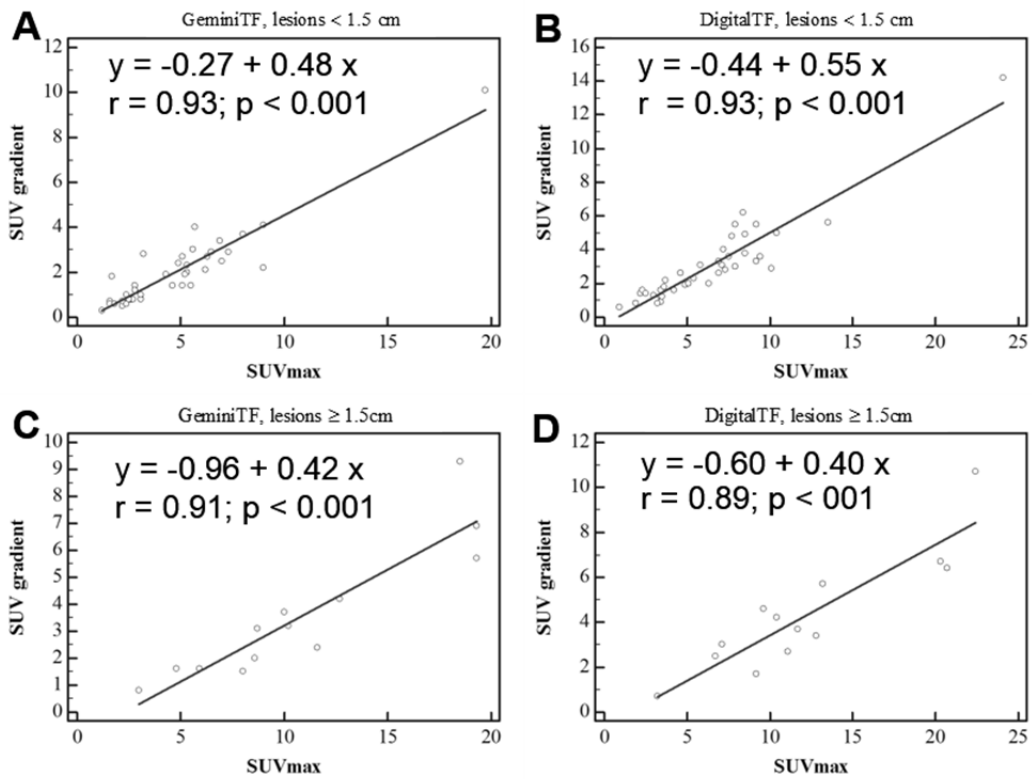
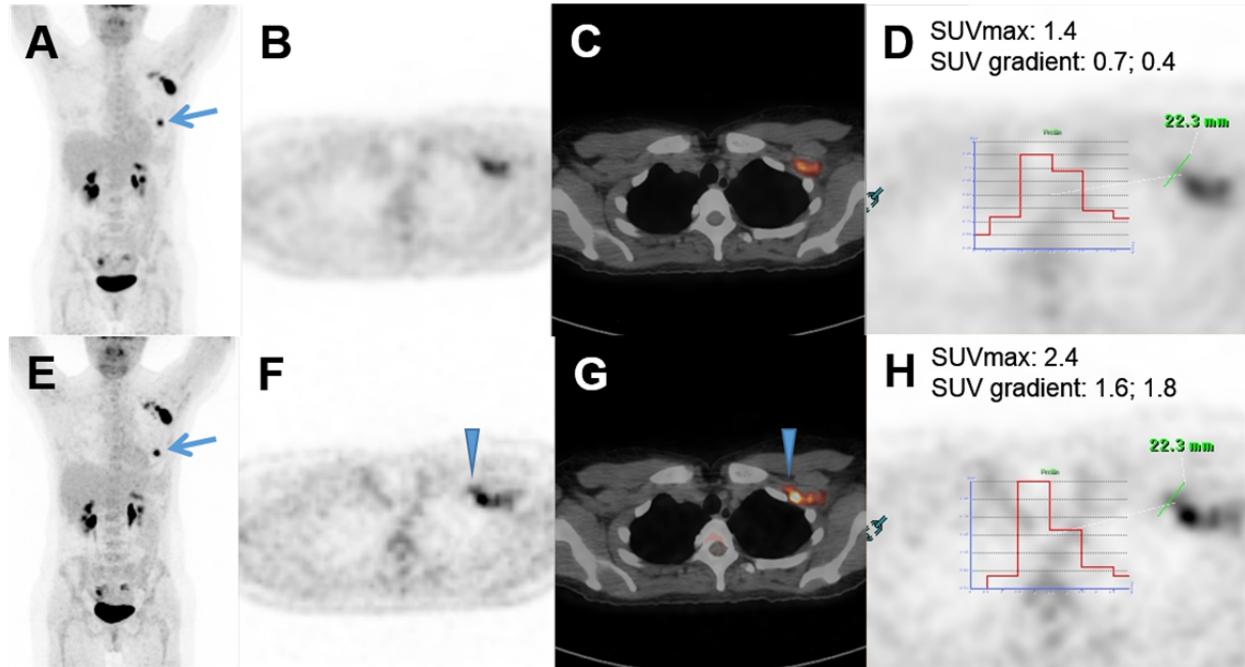


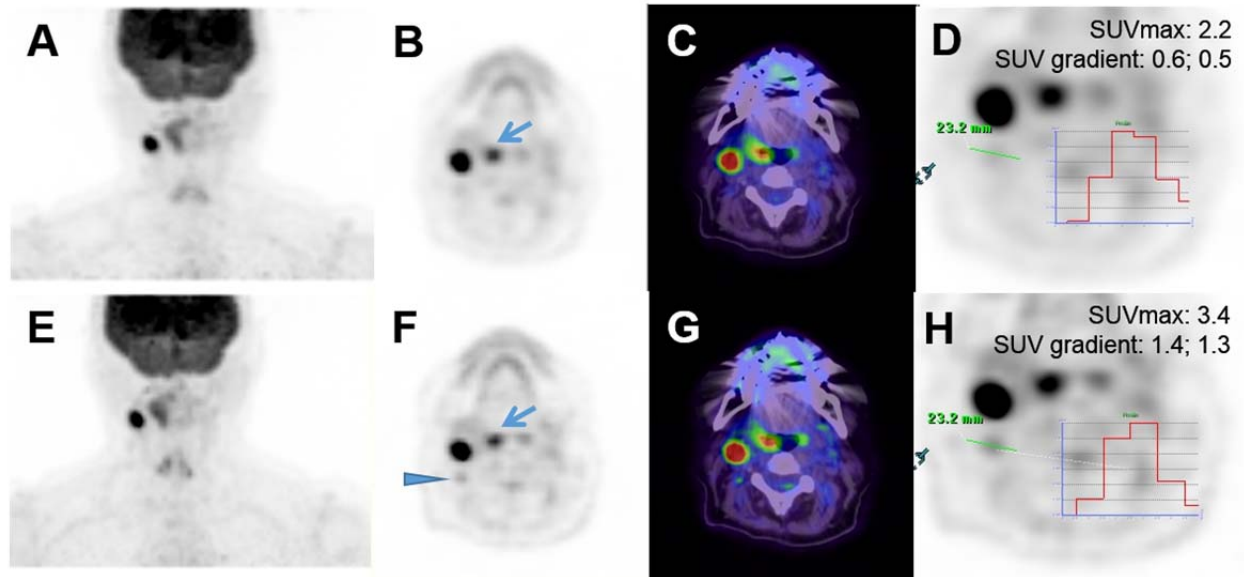
SUPPLEMENTAL DATA TO FIGURES 2-4 IN THE MANUSCRIPT



Supplemental Figure 1. Linear regressions to correlate lesion SUVmax with SUV gradient. A, lesions < 1.5 cm, GeminiTF; B, lesions < 1.5 cm, DigitalTF; C, lesions ≥ 1.5 cm, GeminiTF; lesions ≥ 1.5 cm, DigitalTF. Regression equations with correlation coefficients r and p -values are embedded in the graphs.



Supplemental Figure 2. 47-year-old woman with a history of left breast infiltrating ductal carcinoma for initial staging. GeminiTF images, upper panel: A, maximum intensity projection (MIP) image showing the FDG avid breast primary (arrow); B, axial PET; C, fused axial PET/CT; D, count profile of a level III axillary lymph node. FDG avid lymph nodes were noticed at level I and II of the left axilla, but no FDG avid level III node was diagnosed by both readers. PET/CT staging was T1N1M0 (stage II). DigitalTF images, lower panel: E, MIP image; F, axial PET; G, axial fused axial PET/CT; H, count profile of a level III axillary lymph node. Unlike GeminiTF, the readers identified this additional level III lymph node measuring 0.9 x 1.3 at CT (triangle). PET/CT scanning was T1N2M0 (stage III); no biopsy was obtained for this lesion. This lesion showed greater metabolic activity and sharpness at DigitalTF (H) compared with GeminiTF (D). Subsequent biopsy of a level I axillary node showed evidence of metastasis.



Supplemental Figure 3. 67-year-old woman with a history of right tonsillar squamous cell carcinoma for initial staging. The patient underwent a PET scanning of the torso followed by a regional scanning from mid skull to upper chest for standard of care. The latter body region was scanned again with DigitalTF. GeminiTF images, upper panel: A, maximum intensity projection (MIP) image; B, axial PET showing the FDG avid tonsillar primary (arrow) and an FDG avid lymph node at level IIA, no other FDG avid node was diagnosed; C, fused axial PET/CT findings are consistent with T2N1Mx (stage II); D, count profile of a level IIB cervical lymph node that was missed by GeminiTF. DigitalTF images, lower panel: E, MIP image; F, axial PET; G, fused axial PET/CT; H, count profile of the level IIB cervical lymph node. Unlike GeminiTF, the readers identified this additional FDG avid node at level IIB, measuring 0.6 x 0.6 cm at CT (triangle). PET/CT staging was T2N2Mx (stage III). This node showed greater metabolic activity and sharpness at DigitalTF (H) compared with GeminiTF (D).

SUPPLEMENTAL DATA FOR PHANTOM STUDIES

Methods

Phantom studies were conducted to facilitate a head-to-head comparison of the DigitalTF prototype and the Gemini TF system. In particular, we filled the the IEC phantom using 4:1 spheres:background and scanned it using the A) GeminiTF for 100 s duration, B) DigitalTF for 138 s duration, C) GeminiTF for 334 s duration, and D) DigitalTF for 334 s duration. The whole sequence of 4 scans was repeated 3 times in order to provide insight into the statistical variations. Note that A and B correspond to representative durations used in the clinical scanning. C and D are duration-matched, high-statistics studies appropriate for NEMA evaluation. Results were analyzed by using circular ROIs of the same size as the spheres. The numbers of events were also recorded. The numbers of events were decay corrected to the start time of the first acquisition to produce the plots shown here. Error bars indicate one standard deviation estimated from the triplicates.

As a quantitative measure of lesion conspicuity, we analyzed the data using the NEMA metric percent contrast for hot spheres

$$Q_H = \frac{\frac{\text{Hot Sphere ROI}}{\text{Background ROI}} - 1}{\frac{\text{Hot Sphere Concentration}}{\text{Background Concentration}} - 1}$$

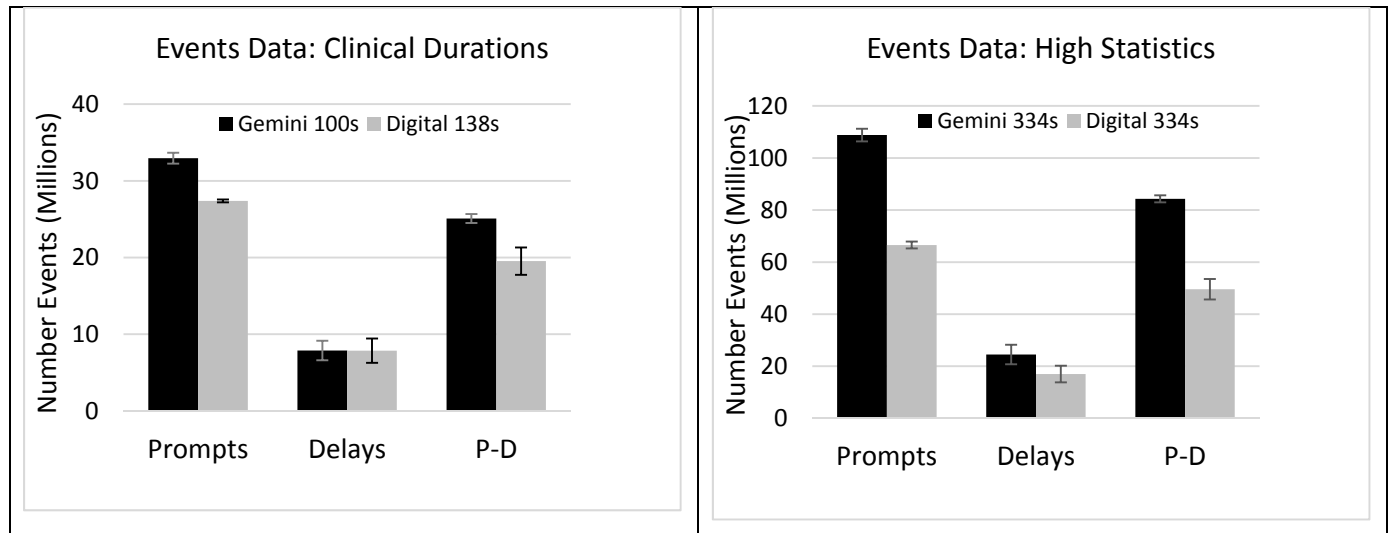
The values in the numerator (ROI) are obtained from the image and those in the denominator (Concentration) obtained from activity measured using the dose calibrator and the fill volumes, precisely determined by mass.

To assess effective spatial resolution achieved under clinical imaging conditions, we reconstructed the phantom images using exactly the same reconstructions as used for the patient scans. We estimated the spatial resolution by fitting a Gaussian kernel blurring model [Kolthammer, *Phys. Med. Biol.* (2014) doi:10.1088/0031-9155/59/14/3843] as a function of sphere size to the RCmax values from the high statistics data.

Results

Number of Events

The DigitalTF collected fewer counts than GeminiTF both using durations representative of clinical scanning and in high statistics studies, Supplemental Figure 4. This behavior is consistent with the lower NEMA sensitivity of the DigitalTF prototype to the GeminiTF. Thus, any image quality advantage of the DigitalTF cannot be simply attributed to having a higher number of events.

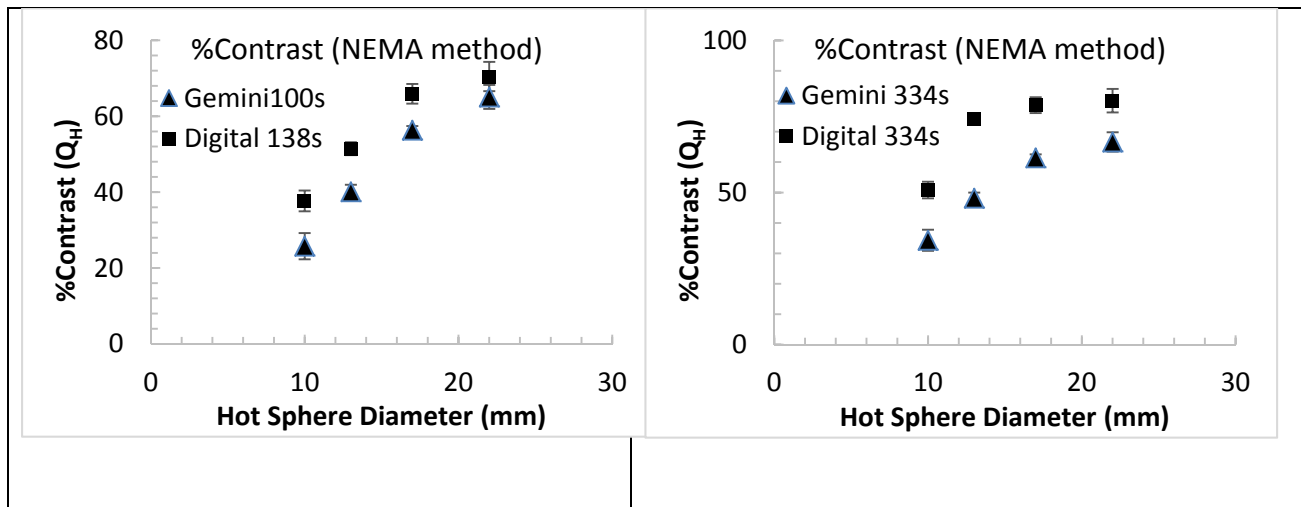


Supplemental Figure 4. Number of events collected using A) durations matched to clinical scanning and B) equal durations.

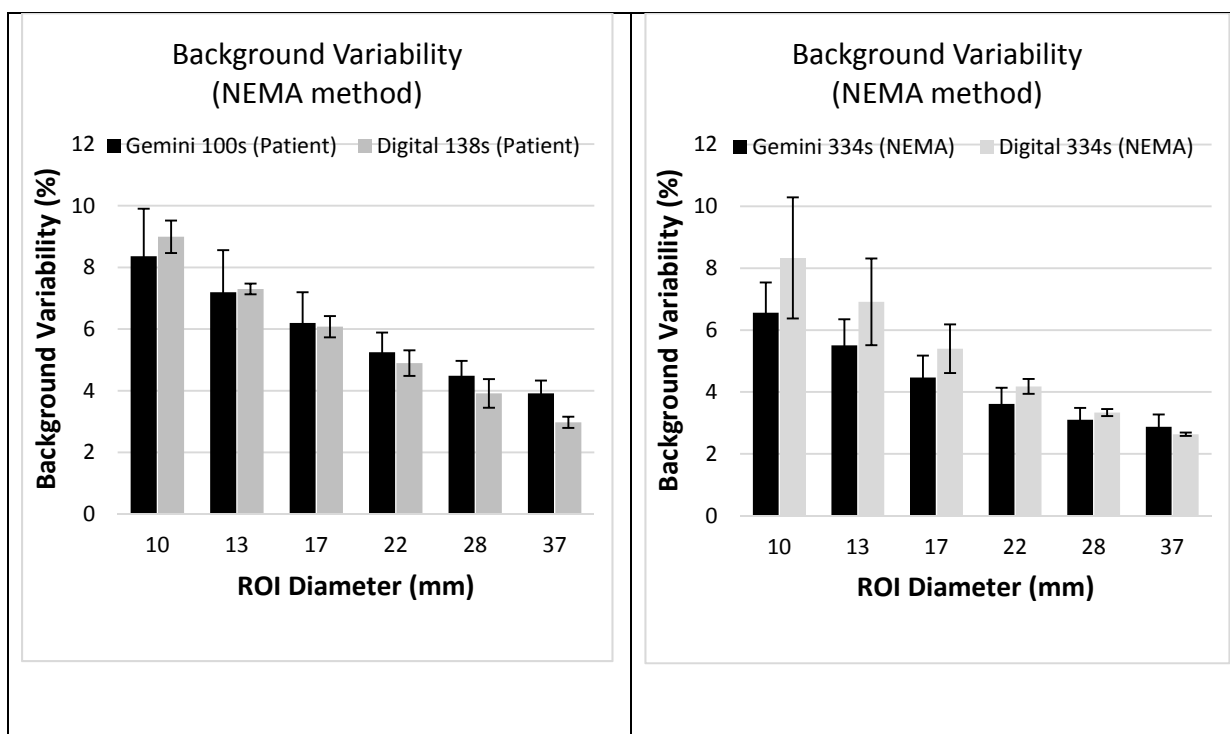
P – D = Prompt minus Delays

NEMA Contrast and Background Variability

Supplemental Figures 5 and 6 show the contrast and background variability in the phantom studies compared for the GeminiTF and the DigitalTF. The NEMA method was followed and results reflect the statistical noise and background nonuniformity. The lower background variability of the GeminiTF, and its greater advantage with matched acquisition durations, might be attributed to having fewer events with the DigitalTF than with the GeminiTF.



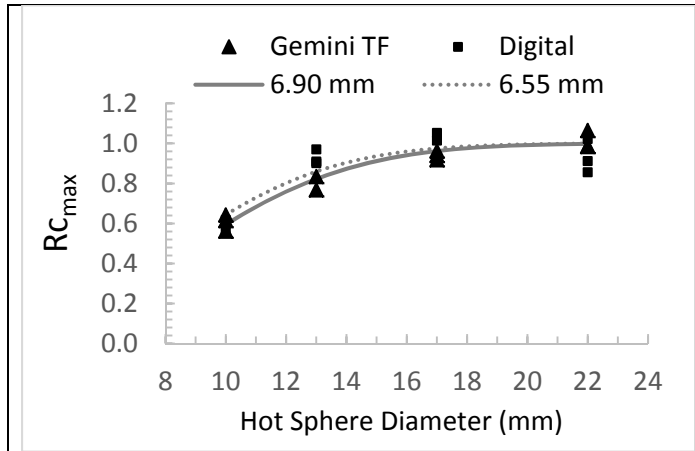
Supplemental Figure 5. Percent contrast determined using A) durations matched to clinical scanning and B) equal durations.



Supplemental Figure 6. Background variability determined using A) durations matched to clinical scanning and B) equal durations.

Spatial Resolution in Clinical Usage

The spatial resolutions were 6.90 and 6.55 mm FWHM for the GeminiTF and DigitalTF respectively, Supplemental Figure 7. Taken together with the NEMA measures of resolution, this indicates that the effect of the clinical reconstruction is to reduce, not enhance, the differences in spatial resolution.



Supplemental Figure 7. RC_{max} versus sphere size and model fits for both the GeminiTF and DigitalTF. The values (symbols) indicate the three measurements for sphere size. The curves indicate the model fits and are labeled with estimated spatial resolution (FWHM) achieved using the clinical reconstruction.